

Annual Review of Physical Chemistry

Photon Upconversion at Organic-Inorganic Interfaces

Zhiyuan Huang,¹ Tsumugi Miyashita,² and Ming Lee Tang³

¹Key Laboratory of Photochemical Conversion and Optoelectronic Materials, Technical Institute of Physics and Chemistry, Chinese Academy of Sciences, Beijing, People's Republic of China; email: huangzhiyuan@mail.ipc.ac.cn

 $^2{\rm Department}$ of Biomedical Engineering, University of Utah, Salt Lake City, Utah, USA; email: tsumugi.miyashita@utah.edu

³Department of Chemistry, University of Utah, Salt Lake City, Utah, USA; email: minglee.tang@utah.edu

Annu. Rev. Phys. Chem. 2024. 75:329-46

The Annual Review of Physical Chemistry is online at physchem.annualreviews.org

https://doi.org/10.1146/annurev-physchem-090722-011335

Copyright © 2024 by the author(s). All rights reserved

Keywords

upconversion, quantum dot, dark exciton, organic-inorganic interface, triplet energy transfer, triplet-triplet annihilation

Abstract

Photon upconversion is a process that combines low-energy photons to form useful high-energy photons. There are potential applications in photovoltaics, photocatalysis, biological imaging, etc. Semiconductor quantum dots (QDs) are promising for the absorption of these low-energy photons due to the high extinction coefficient of QDs, especially in the near infrared (NIR). This allows the intriguing use of diffuse light sources such as solar irradiation. In this review, we describe the development of this organic-QD upconversion platform based on triplet-triplet annihilation, focusing on the dark exciton in QDs with triplet character. Then we introduce the underlying energy transfer steps, starting from QD triplet photosensitization, triplet exciton transport, triplet-triplet annihilation, and ending with the upconverted emission. Design principles to improve the total upconversion efficiency are presented. We end with limitations in current reports and proposed future directions. This review provides a guide for designing efficient organic-QD upconversion platforms for future applications, including overcoming the Shockley-Queisser limit for more efficient solar energy conversion, NIR-based phototherapy, and diagnostics in vivo.

QD: quantum dot

light-emitting diode

TTA: triplet-triplet

photoluminescence

UC: upconversion

OLED: organic

NC: Nanocrystal

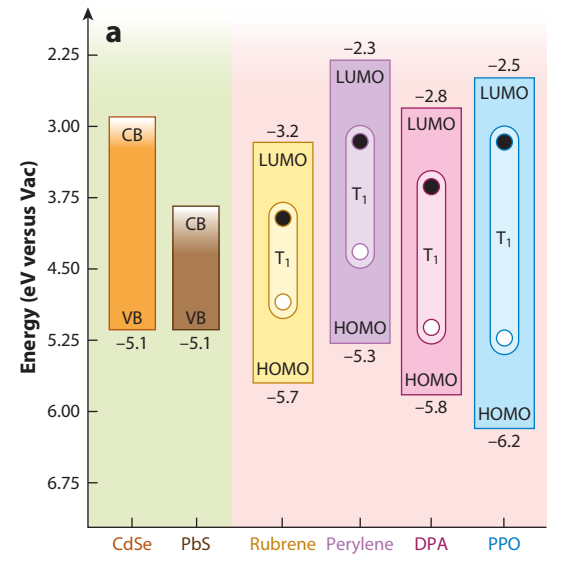
annihilation

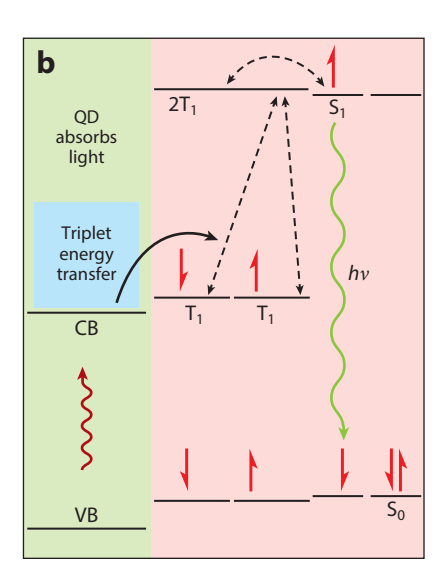
PL:

1. INTRODUCTION

The radiative recombination of excitons from conjugated organic molecules and quantum dots (QDs) can produce light of arbitrary wavelength. Light emitted from this class of materials, e.g., by organic light-emitting diodes (OLEDs) and QDs, can be higher in color purity and isotropic in direction compared to older technology, factors contributing to high-quality displays. Clearly, emission from these bright excitons can be used for energy conversion, but what about the dark excitons? Due to considerable electron-hole Coulomb interactions, the Frenkel excitons in organic semiconductors and semiconductor nanocrystals (NCs) are characterized by a large binding energy of ~0.5 eV, compared to the 10-meV binding energy for the hydrogenic Mott-Wannier excitons in bulk semiconductors. This strong Coulombic interaction results in a sizeable spinexchange energy in these materials and introduces a dark triplet excited state lower in energy than the singlet state. Though triplet excitons are classically forbidden from emitting light, a pair of triplet excitons that have a net spin of zero can be fused into two singlet excitons, both of which can strongly couple to light. This process is known as triplet-triplet annihilation (TTA). Here, we review the development of organic-QD hybrid nanomaterial systems for energy conversion using the Frenkel excitons in organic semiconductors and QDs (Figure 1a). Moving beyond Stokesshifted photoluminescence (PL) from the bright singlet excitons in these materials, we focus on photon upconversion (UC) with dark triplet excitons. Photon UC is a process where low-energy photons are combined to produce one high-energy photon, which could potentially be applied

in photovoltaics, photocatalysis, phototherapy, etc. (Figure 2). In particular, we concentrate on





(a) Band edge positions of CdSe and PbS QDs that absorb light for photon upconversion for triplet energy transfer to the emitter molecules rubrene, perylene, DPA, and PPO. The energetics of the frontier orbitals and lowest excited triplet state are illustrated. (b) Schematic of the energy transfer during photon upconversion with QD triplet photosensitizers and subsequent triplet-triplet annihilation. Abbreviations: CB, conduction band; DPA, 9,10-diphenylanthracene; HOMO, highest occupied molecular orbital; LUMO, lowest occupied molecular orbital; PPO, 2,5-diphenyloxazole; QD, quantum dot; Vac, vacuum; VB, valence bond.



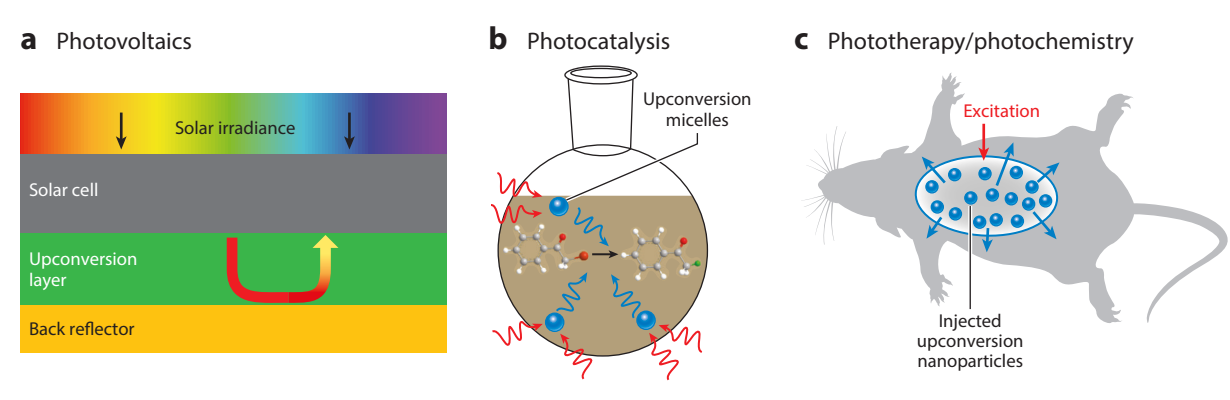


Figure 2

Illustrations showing applications of photon upconversion in (a) photovoltaics, (b) photocatalysis, and (c) phototherapy/photochemistry.

photon UC via TTA. As shown in **Figure 1***b*, TTA is an energy-conserved, spin-allowed process where two spin-triplet excitons originally in separate molecules can combine, resulting in one of the molecules excited to an emissive singlet state. Note that the average smartphone user may unwittingly be familiar with TTA: TTA is already used to improve the external quantum efficiency of the blue OLEDs (1). TTA recycles the three dark triplet excitons that are created with each bright singlet exciton that results from electrical injection (2). TTA raises the maximum internal quantum efficiency of fluorescent OLEDs from 25% (that rely solely on emission from singlet excitons) to 62.5% (3).

The primary advantage of TTA over other photon UC methods is the fact that classically allowed, real states are utilized for energy conversion. In practical terms, this allows TTA-based photon UC to occur with diffuse sources of light, e.g., sunlight (4, 5). In general, the forbidden optical transitions and low absorption cross sections in the lanthanides mean expensive pulsed or high-power lasers are normally used for excitation. For example, state-of-the-art lanthanide nanoparticles optically triggering neurons deep in the mouse brain caused the temperature at the surface of the mouse skull to reach 43.3°C, nearly approaching the cytotoxic threshold of 45°C (6). This is directly related to the fact that the molar extinction coefficients, ε , of the isolated lanthanide ions are <10 M⁻¹cm⁻¹, up to 10,000 times smaller than molecular or NC light absorbers (7, 8).

Upconverted emission is proportional to the system's ability to both absorb and emit photons. This is quantified by the quantum efficiency (QE) term, where QE = $\varepsilon \bullet \Phi_{PL}$. The molar extinction coefficient ε is directly proportional to light absorption at each wavelength and Φ_{PL} is the UC PL quantum yield (QY). The QE term clearly shows that a high fluorescence QY is for naught if absorption is negligible. For example, indocyanine green (9), the brightness benchmark for near-infrared (NIR) contrast agents, has a QE_{max} = 1,350 M⁻¹cm⁻¹ at 800 nm. State-of-the-art lanthanide nanoparticles have a QE_{max} = 0.25 M⁻¹cm⁻¹ given their reported Φ_{PL} = 2.5%. In contrast, we have shown QE = 7,200 M⁻¹cm⁻¹ and 3,000 M⁻¹cm⁻¹, respectively, for the UC of green to violet and NIR to yellow light with CdSe and PbS QDs, respectively. The QE with semiconductor QDs for photon UC vastly exceeds the QE with lanthanides by five orders of magnitude.

In this review, we outline the historical development of photon UC at organic-inorganic interfaces, the factors affecting the QE of this multistep energy transfer process, and finally, the prospects and challenges that need to be addressed.

QE: quantum efficiency QY: quantum yield NIR: near infrared **TET:** triplet energy

transient absorption

transfer

TA:

2. BACKGROUND

2.1. Molecular Triplet Sensitization: From Heavy Metal Porphyrins to Quantum Dots

The first report of QD-based photochemical UC in 2015 built heavily on lessons derived from the molecular world. TTA was initially observed by Parker et al. (10, 11) in 1962 on a phenanthracene donor/naphthalene acceptor system. The field lay dormant until 2003 when Baluschev and colleagues (12, 13) used metal(II)-octaethyl porphyrins to sensitize conjugated polymers. Many groups around the world built on this, e.g., to extend photosensitizer absorption to the NIR via increasing the conjugation length of the porphyrin (14) or introducing metal to ligand charge transfer transitions (15). Important insights on the kinetics of TTA were derived by Monguzzi, Meinardi, and colleagues (16) and Schmidt & Castellano (17). This allowed experimental observables like the excitation density required for the transition from the linear to the quadratic regime for TTA to be related to the intrinsic photophysical properties of the molecules involved (for further elaboration see Section 3).

The first observation of triplet energy transfer (TET) between NCs and molecules were two independent publications in 2014 by Rao and colleagues (18) and Bawendi and Baldo (19), respectively. Both papers showed that triplet excitons produced via singlet fission in acenes were transferred to lead chalcogenide NCs. This was a paradigm shift because the field of semiconductor NCs had focused solely on Förster resonance energy transfer in the preceding 30 years despite the fact that it was well known that the lowest excited state in colloidal NCs had dark, triplet-like character (20) (Figure 3). In 2014, Baldo and Bawendi (19) reported enhanced PL of PbS NCs due to the downconversion of singlets formed in tetracene, and subsequent TET to the PbS acceptors (19). Using transient absorption (TA) spectroscopy, Rao and colleagues (18) showed that triplets derived from singlet fission migrated from pentacene to PbSe NCs, followed by backwards hole then electron transfer from the NCs to the acene. These studies motivated efforts to demonstrate the reverse processes, that is TET from NCs to molecules. CdSe and PbS/PbSe NC sensitized photochemical UC in solution was the focus of the first publications on the photosensitization of triplet excitons from inorganic semiconductor NCs. Later, Wu et al. (21) reported photon UC based on PbS NC light absorbers in thin film. In terms of mechanistic studies, Mongin et al. (22) reported the formation of triplet excitons on pyrene and anthracene ligands bound to CdSe NCs

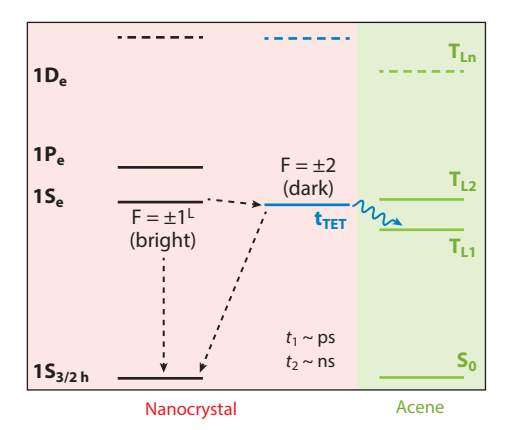


Figure 3

The sensitization of molecular triplet states $(T_{L1},T_{L2},\ldots,T_{Ln})$ from the dark triplet-like $F=\pm 2$ state in quantum dots.

upon photoexcition of the CdSe component. These TA experiments directly showed evidence of TET from inorganic NCs to bound organic ligands.

There is unequivocal evidence for the QD sensitization of molecular triplet states. From spin conservation arguments, it is expected that the dark excitonic state in the QD, a few millielectron volt below the lowest excited bright singlet state, is responsible for transferring triplets to molecules. The lifetimes of the bright and dark state, and $\Delta E_{\rm ST}$, the energy difference between these two states, can be obtained via low temperature time-resolved PL and TA experiments (23–28). This small $\Delta E_{\rm ST}$ minimizes losses in triplet photosensitization for photon UC and is one of the advantages of using QDs for absorbing light. Interestingly, at low temperatures around 5–40 K, Lian and coworkers (29) found evidence of the bright state in CdSe/CdS core/shell nanoparticles photosensitizing the triplet state of surface-bound sexithiophene. This is because triplet transfer coupling matrix elements are nonzero for all exciton states (whether bright or dark) in the QD as they have the same electron/hole spin projections.

The Dexter description of TET is a two-electron exchange integral (30). Thus, direct TET between QDs and organics can occur by superexchange via virtual states for the simultaneous transfer of both the hole and electron (31-34), or sequentially via charge separated intermediates (35, 36). The dominant mechanism depends on the nature of the QD surface and the atomic details of the interface. QDs with more dangling bonds or surface trap states likely bias TET towards charge-separated intermediates. The general expression invoking the Born-Oppenheimer approximation describing nonadiabatic energy transfer is given by the Fermi golden rule, $k_{\text{TET}} = \frac{2\pi}{\hbar} \cdot |H_{\text{DA}}|^2 \cdot \rho(E_{\text{f}})$, where $|H_{\text{DA}}|^2$ is the electronic coupling matrix squared and $\rho(E_{\text{f}})$ is the Franck-Condon factor-weighted density of states. $|H_{DA}|^2$ depends on the electronic coupling between the molecular donor and NC acceptor and $\rho(E_{\rm f})$ on the overlap of the nuclear wave functions of phonon and vibrational modes before and after energy transfer. If $|H_{\rm DA}|^2$ is large, then energy transfer in this hybrid system is adiabatic. Marcus theory (37) (Equation 1) is one possible description of the rate of nonadiabatic energy transfer, where $k_{\rm ET}$ is proportional to the driving force, or the energy offset between the triplet states of the NC acceptor and molecular donors, ΔG^0 , and a prefactor that takes into account the frequency of surmounting the energetic barrier where the donor and acceptor cross

$$k_{\text{TET}} = \frac{2\pi}{\hbar} \cdot |H_{\text{DA}}|^2 \cdot \frac{1}{\sqrt{4\pi\lambda k_{\text{B}}T}} \exp\left(-\frac{(\lambda + \Delta G^0)^2}{4\lambda k_{\text{B}}T}\right).$$
 1.

In related work, Olshansky and Alivisatos (38) have estimated $\lambda \sim 0.4-0.5$ eV for hole transfer from CdSe-CdS core-shell NCs to surface bound ferrocene.

Equilibration of the triplet excited state between NCs and the surface bound molecules has been described by the same model for molecules displaying thermally activated delayed fluorescence (TADF). TADF molecules have a small $\Delta E_{\rm ST}$ that allows intersystem crossing and reverse intersystem crossing to occur within the same molecule that is spatially carved into donor-acceptor regions (39, 40). Temperature-dependent PL measurements show that the $\Delta E_{\rm ST}$ term related to the exchange energy in TADF molecules is interchangeable with $\Delta E_{\rm GAP}$, the energy difference between the QD excited state and the lowest excited triplet state on the molecule. For example, pyrene functionalized CdSe NCs (22) and quinoline and naphthalene functionalized InP nanoparticles (41, 42) exhibit thermally activated delayed photoluminescence whereby the nanoparticle lifetimes are extended from tens of nanoseconds to hundreds of microseconds. This is analogous to the delayed fluorescence in TADF molecules and is attributed to the long-lived molecular triplet exciton toggling back and forth between the organic and NC.

TADF: thermally activated delayed fluorescence

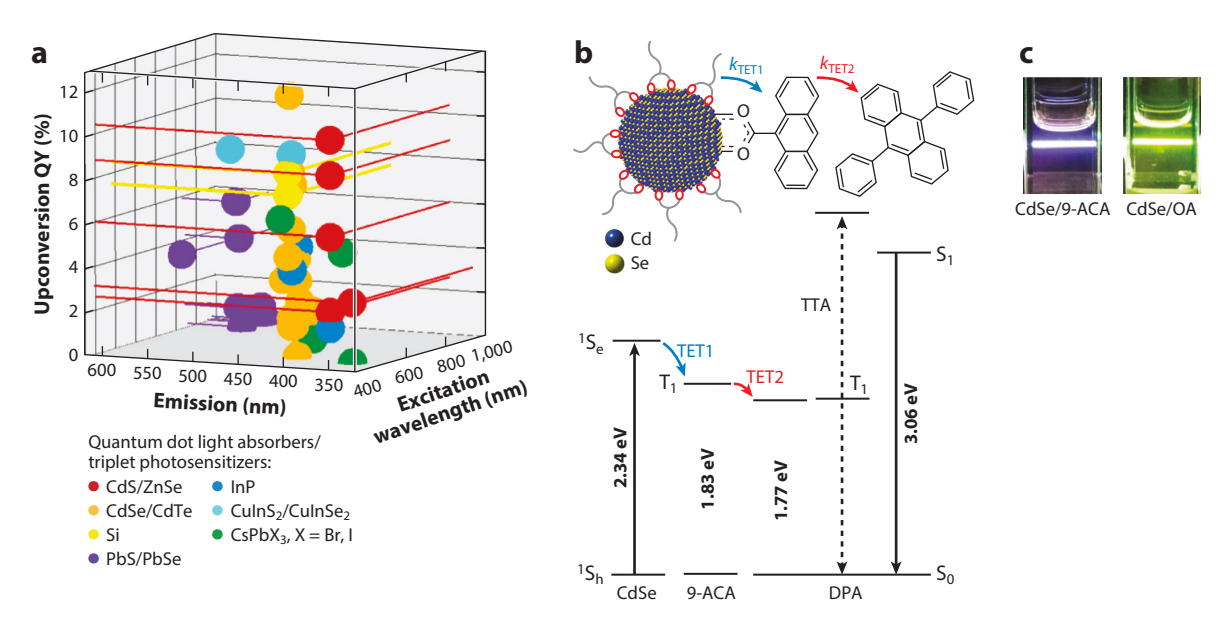


Figure 4

(a) The photon upconversion QY (maximum of 50%) is plotted with respect to the excitation and emission wavelengths. Different quantum dot light absorbers are distinguished by color. (b) The energy diagram for CdSe/9-ACA sensitized photon upconversion with DPA annihilator molecules. (c) A transmitter ligand (e.g., 9-ACA) is critical in promoting the orbital overlap necessary for efficient Dexter transfer. Without this ligand, photon upconversion is 1,000 times weaker; i.e., no violet light is produced from green light under the same conditions. Abbreviations: 9-ACA, 9-anthracene carboxylic acid; DPA, 9,10-diphenylanthracene; QY, quantum yield; TTA, triplet-triplet annihilation.

2.2. Transmitter Ligands Are Essential for Efficient Photon Upconversion

Figure 4*a*'s ummarizes the QDs that have been used for photon UC with molecular emitters (5, 21, 31, 33, 34, 36, 42–79) in terms of the photon UC QYs (out of a maximum of 50%). As observed from the clustering in the emission wavelengths, the field is limited to certain emitter molecules, specifically rigid molecules (**Figure 1***a*) that have the suitable energetics for efficient TTA, i.e., $2T_1$ slightly larger than S_1 . Broadly speaking, with $T_1 \sim 1.1$ eV (80), rubrene is used for NIR to yellow photon UC with lead chalcogenide and CuInSe₂ QDs. Perylene and 9,10-diphenylanthracene (DPA), with $T_1 \sim 1.5$ eV and 1.8 eV; respectively (80), are used for green- or red-to-violet UC with CdTe, CdSe, InP, perovskite, and CuInS₂ silicon QDs. Finally, blue-to-ultraviolet photon UC occurs with large band gap QDs like CdS and ZnSe since emitter molecules in the UV [e.g., 2.5-diphenyloxazole (PPO) and 1,4-bis((triisopropylsilyl)ethynyl)naphthalene (TIPS-Nph)] are relatively inefficient in terms of TTA because of their energetic triplet states and low fluorescence QYs. The largest anti-Stokes shift reported so far is green to UV photon UC using perovskite NCs and TIPS-Nph (53).

Surface bound transmitter ligands are key to the efficient spin-triplet exciton photosensitization necessary for high photon UC QYs. Typically, a transmitter has a conjugated core that is similar to the emitter, so the triplet state of transmitters are close to that of the emitters. This guarantees efficient energy transfer from QDs to the emitters. In addition, the close binding of transmitters to QD surfaces ensures intimate orbital overlap between the donor and acceptor for optimal wave function distribution between the QD triplet photosensitizer and the organic emitter. For example, in **Figure 4b**, we show that the 9-anthracene carboxylic acid (9-ACA) transmitter enhances CdSe sensitized photon UC by 3 orders of magnitude (70) whereby a green

DPA: 9,10-diphenylanthracene

PO:

2,5-diphenyloxazole

TIPS-Nph: 1,4-bis((triisopropylsilyl)-ethynyl)naphthalene

9-ACA: 9-anthracene carboxylic acid

continuous-wave laser produces violet emission, whereas the same experiment in the absence of a transmitter ligand mainly results in green CdSe QD PL and scatter of the green laser.

3. DESIGNING AN EFFICIENT ORGANIC QUANTUM DOT UPCOVERSION PLATFORM

In this section, we describe the various factors affecting photon UC in this hybrid system.

3.1. Theoretical Background

The measured photon UC efficiency allows us to account for the losses during TET and TTA. For the three-component UC platform comprising a QD sensitizer, transmitter, and emitter, η_{UC} is described by the following equation:

$$\eta_{\rm UC} = f \times \eta_{\rm TET1} \times \eta_{\rm TET2} \times \eta_{\rm TTA} \times \eta_{\rm F},$$
2.

where f is the spin statistical factor defining the fraction of excited emitter triplets that produce a singlet excited state via TTA. η_{TET1} , η_{TET2} , η_{TTA} , and η_{F} are the efficiencies of TET from triplet photosensitizer to the transmitter, TET from the transmitter to the emitter (**Figure 4b**), TTA, and emitter fluorescence, respectively. All the terms in Equation 1 have a maximum value of 1, with the exception of Φ_{TTA} , which is capped at 0.5. The TTA efficiency Φ_{TTA} is affected by k_{T} and k_{TTA} :

$$\eta_{\text{TTA}} = \frac{k_{\text{TTA}}[^3 A^*]}{2k_{\text{TTA}}[^3 A^*] + k_{\text{T}}}.$$
3.

With the factor of 2 in the denominator in Equation 3, the maximum η_{TTA} equals 0.5. Thus, the maximum η_{UC} equals 0.5.

3.2. Quantum Dot Design

As the photoexcited donor effects triplet energy transfer, the photon UC quantum yield, and efficiency of TET to the transmitter/acceptor, molecules are affected by the QD size, morphology, and energetic distribution of defect states. Below we discuss these factors in detail.



- **3.2.1.** Size. η_{TET1} , the efficiency of TET from QDs to transmitters, is correlated with QD size. TET is the correlated or sequential transfer of both electrons and holes, and the rate follows Marcus theory, contingent upon the driving energy (37), in this case the QD-transmitter triplet energy offset. Therefore, small QDs with a large driving force for TET are preferred for fast and efficient TET (35, 36, 81). This size dependence has been experimentally proven with different kinds of QDs. In green-to-violet UC, when the diameters of wurtzite CdSe QDs vary from 2.7 to 5.1 nm, the corresponding η_{UC} decreases from 7.5% to 0.26% (**Figure 5***a*) (71); the same size dependence was observed in zinc-blende CdSe QDs where the k_{TET1} obtained from TA dropped from 59.8 ns⁻¹ to 6.74 × 10⁻⁵ ns⁻¹ with the increase of the QD radius from 1.20 to 2.66 nm (72). For NIR-to-visible UC, η_{UC} is impacted by the size of PbS(Se) QDs by a factor of 700 (67). It is worth noting that the efficient TET1 and UC with small QDs comes at the price of the energy loss rendering a smaller anti-Stokes shift.
- **3.2.2. Morphology.** Other than zero-dimensional QDs, one-dimensional nanorods and two-dimensional nanoplatelets can sensitize UC. The anisotropic nature of nanorods and nanoplatelets makes it possible to deduce if TET at organic-inorganic interfaces is directional or polarization related. In 2020, the Nienhaus group (55) first reported triplet photosensitization by nanoplatelets. As shown in **Figure 5***b*, CdSe nanoplatelets combined with 9-ACA transmitters and DPA emitters upconvert green-to-violet light. In comparison with CdSe QDs under the same conditions,

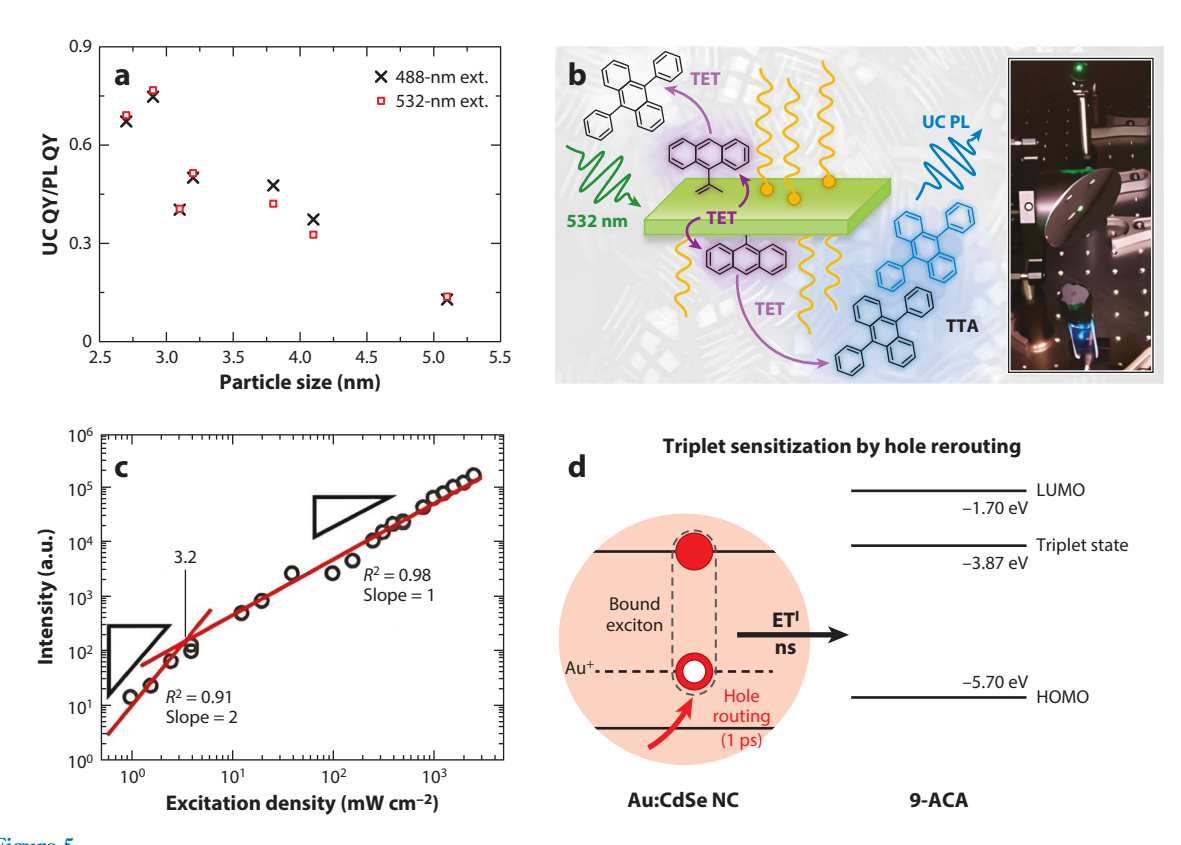


Figure 5

(a) The dependence of green-to-violet UC on the size of CdSe QDs. (b) Green-to-violet UC sensitized by CdSe nanoplatelets. (c) The power dependence of near-infrared-to-visible UC sensitized by PbS/CdS core-shell QDs. (d) The hole rerouting effect in TET from Au-doped CdSe NCs to surface anchored 9-ACA. Abbreviations: 9-ACA, 9-anthracenecarboxylic acid; HOMO, highest occupied molecular orbital; LUMO, lowest occupied molecular orbital; NC, nanocrystal; PL, photoluminescence; QDs, quantum dots; QY, quantum yield; TET, triplet energy transfer; TTA, triplet-triplet annihilation; UC, upconversion. Panel a adapted with permission from Reference 71; copyright 2015 American Chemical Society. Panel b adapted with permission from Reference 55; copyright 2020 American Chemical Society. Panel c adapted with permission from Reference 56; copyright 2020 John Wiley & Sons, Inc.

CdSe nanoplatelets exhibit a larger absorption cross section that allows for a lower concentration of sensitizers during UC. Additionally, the sharper emission of nanoplatelets compared to QDs indicates that the inhomogeneous broadening is minimized because the exciton energy is only determined by platelet thickness. Nonetheless, the total $\eta_{\rm UC}$ is only 4.6%, less efficient than the 8.0% for QDs. This is explained in a follow-up study (43) from the same group: Nanoplatelets easily stacked, and triplets of surface-anchored 9-ACA tend to annihilate to singlets instead of transferring to DPA. However, not only are 9-ACA singlets less emissive than DPA, but they can be quenched by the CdSe nanoplatelet, resulting in inefficient UC. This argument also applies to nanorods that upconvert red light to blue with an efficiency of 2.1% (52). Perhaps a bulky transmitter ligand is needed for nanoplatelet and nanorod sensitized UC systems to avoid molecular stacking/aggregation in order to obtain UC efficiencies comparable to spherical QDs.

3.2.3. Defect-mediated triplet energy transfer. In semiconductor QDs, lattice imperfections such as atomic vacancies, impurities, or surface dangling bonds may introduce exciton traps that

modify the dynamics of energy or charge transfer from QDs to acceptors. Specifically, while TET might be slowed down by the fast trapping of electrons, holes, or both, the total $\eta_{\rm UC}$ can be enhanced or diminished (46, 82). Below, we discuss the role of defects in TET and UC.

Typically, intrinsic defects such as surface dangling bonds or lattice vacancies are widely distributed in energy and vary from sample to sample. These are challenging to control experimentally and are detrimental to TET and UC. It has been reported that $\eta_{\rm UC}$ is positively correlated with the PL QYs of QDs (71). This suggests that defect-induced nonradiative recombination is one of the decay pathways that competes with TET. Besides, the defect states trap the excitons and slow down TET1. Jin & Lian (83) showed that the rate of TET from CdSe QDs to the surface anchored 9-ACA is 13–37 times slower for trap excitons than band edge excitons depending on the energy levels of the defect states. Since the surface defects can be effectively passivated by inorganic shells, a series of core-shell QDs have been used to promote TET and UC (45, 49, 65, 66, 84). For example, the growth of a CdS shell enhances the $\eta_{\rm UC}$ of PbS QD sensitized NIR-to-visible UC by a factor of 1.43 (34). This increase in $\eta_{\rm UC}$ is attributed to the enhanced $\eta_{\rm TET1}$ due to the suppression of hole transfer from PbS QDs by the CdS shell. Additionally, PbS/CdS core-shell QDs reduce the UC threshold intensity down to 3.2 mW/cm², three times lower than the solar flux (**Figure 5***c*) (5). This allows QD-sensitized UC to be operable under solar flux and potentially applied in solar energy conversion.

In comparison, extrinsic defects that are well controlled in energetics by doping or surface adsorption can facilitate TET and UC. A fast trapping of excitons by these dopant-induced defect states circumvents electron-hole recombination and generates long-lived trapped excitons for subsequent TET to transmitters. In 2020, Ronchi et al. (56) reported Au-doped CdSe QDs can sensitize green-to-violet UC, with η_{TET1} close to unity. They reported the record efficiency of QD-sensitized UC of 12%. This is due to the hole rerouting effect shown in (**Figure 5d**): Efficient hole capture by the Au⁺ state and long-lived trapped excitons enable loss-free TET to 9-ACA transmitters. Other than doping, Mahboub et al. (61) showed that surface states on PbS QDs created by the adsorption of Cd²⁺ and Zn²⁺ can mediate TET by exciton trapping, resulting in 700- and 325-fold enhancements in η_{UC} ; Han et al. (60) also presented that CuInS₂ QDs with excitons self-trapped into Cu-related states result in a 92.3% TET efficiency despite a relatively slow rate of TET.

3.3. Transmitter Design

As the first molecular acceptor during the initial step of energy transfer, the efficiency of TET from the QD donor is affected by transmitter ligand surface coverage, its distance from the surface of the QDs, and its binding group. Below we discuss these factors in detail.

3.3.1. Surface coverage. The surface coverage of transmitter ligands, n, plays a key role in determining η_{UC} . As presented in **Figure 6**n, the UC intensity initially increases with n and then drops if n goes beyond the optimum (69). While the rate and efficiency of TET1 increase with n, the efficiency of TET2 may decrease if n is too high. This is because densely packed transmitters lead to intermolecular interactions such as excimer formation or TTA of transmitters on the surface of the QD (66), which hinders the transfer of transmitter triplets to emitters. Though the annihilation of two triplets in the transmitter ligands generates a bright singlet state, close proximity to the QD leads to a quick reabsorption of the transmitter exciton. In addition, the emission from the transmitter singlet state is not efficient because the fluorescence QYs of transmitters are typically lower than that of emitters (85). An aforementioned example is that the hypothesized TTA of 9-ACA transmitter ligands when nanoplatelets sensitizers stack, resulting in a much lower η_{UC} (43). Another explanation of the $\eta_{\text{UC}-n}$ relationship is that the strong electronic coupling

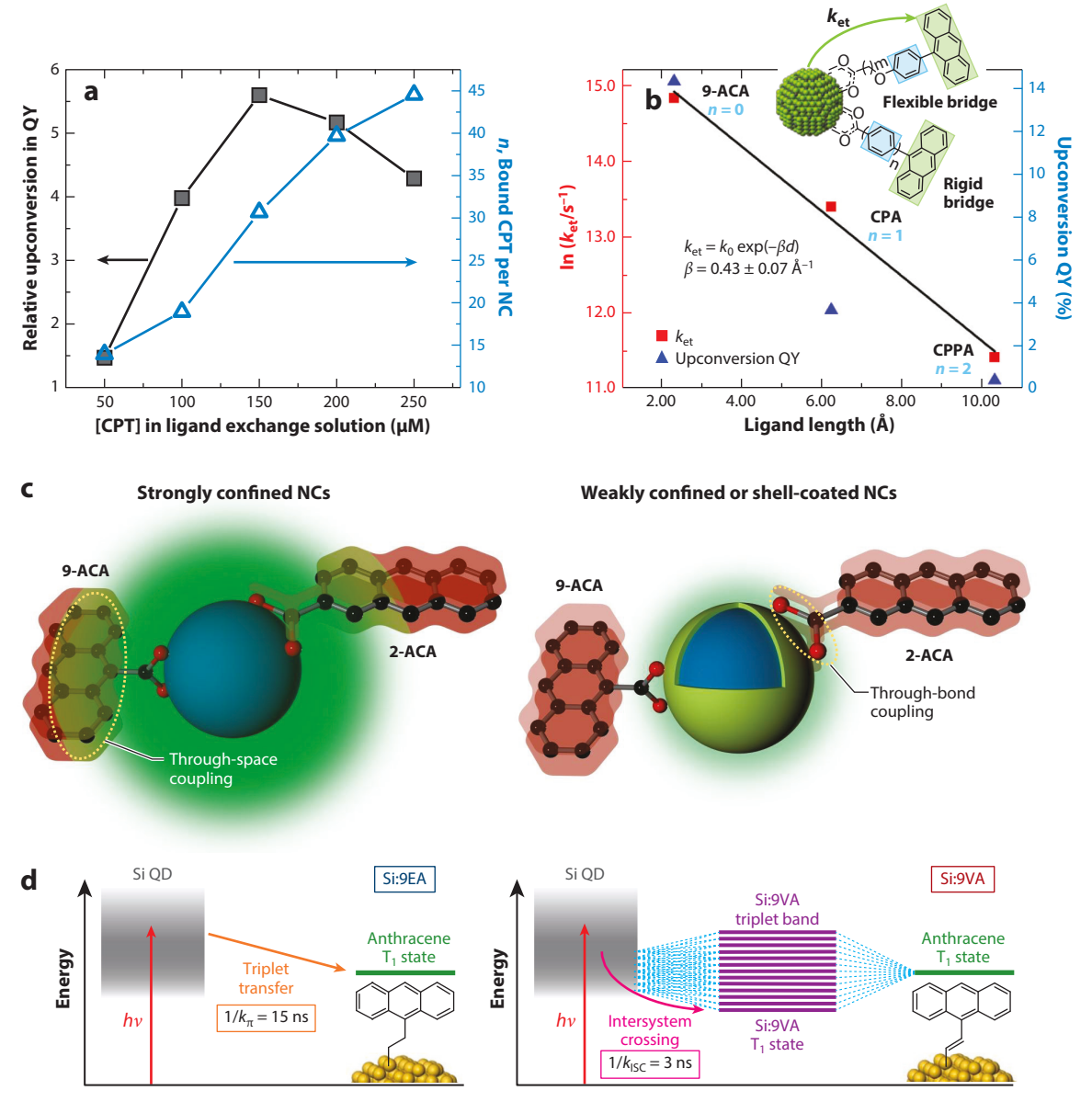


Figure 6

(a) The dependence of the UC intensity on the surface density of tetracene-based transmitter ligands on PbS QDs. (b) Damping coefficients of triplet energy transfer from CdSe QDs to anthracene with aromatic and aliphatic bridges. (e) Two scenarios of QD (NC in this figure)-transmitter coupling: through-space coupling for strongly confined QDs and through-bond coupling for weakly confined QDs. (d) Si QDs are weakly coupled with anthracene through C-C and strongly coupled through C=C bond due to the hybridization of valence states. Abbreviations: 9-ACA, 9-anthracene carboxylic acid; CPA, 4-(anthracen-9-yl)benzoic acid; CPPA, 4'-(anthracen-9-yl)-[1,1'-biphenyl]-4-carboxylic acid; CPT, 4-(tetracen-5-yl)benzoic acid; NCs, nanocrystals; QDs, quantum dots; QY, quantum yield; UC, upconversion. Panel a adapted with permission from Reference 69 (CC BY-NC 3.0). Panel b adapted with permission from Reference 68; copyright 2016 American Chemical Society. Panel c adapted with permission from Reference 57; copyright 2020 John Wiley & Sons, Inc. Panel d adapted with permission from Reference 47; copyright 2023 Springer Nature Limited. between transmitters and QDs can induce excimer formation or partial hybridization (47). The increase of *n* shifts the hybridized triplet states to lower energy that is not energetically favorable for TET2 (**Figure 6***d*).

2-ACA: 2-anthracene carboxylic acid

3.3.2. QD-transmitter spatial separation. The distance between QDs and transmitters determines the rate of TET, which is correlated with η_{TET1} . However, closer or faster is not always better for η_{UC} . A fast TET1 and high η_{TET1} may be accompanied by a low η_{TET2} . Gray et al. (50) studied UC sensitized by PbS QDs with four tetracene-based transmitters that are energetically and structurally similar. Despite having the largest QD-transmitter distance and the slowest QD-to-transmitter TET among all four transmitters, the tetracene derivative with benzoic acid at the 5-position shows the highest η_{UC} thanks to this molecule having the longest triplet lifetime that is beneficial to TET2. The same conclusion was reported by Xu et al. (33, 86), wherein the triplet of transmitters closely bound to PbS QDs are quenched by the heavy atom effect and result in a low η_{TET2} . Therefore, the QD-transmitter distance must be controlled to balance η_{TET1} and η_{TET2} for an optimal η_{UC} .

The design of transmitters with an optimal QD-transmitter distance requires understanding the dependence of k_{TET1} on distance. As the TET between QDs and organic molecules follows a Dexter-like mechanism (19, 32, 33, 63, 68, 87), there is an exponential distance dependence (**Figure 6b**) described as

$$k_{\text{TFT1}} = k_0 e^{-\beta d}$$
,

where k_0 is the prefactor, d is the QD-transmitter distance, and β is the damping coefficient. β is contingent upon the coupling between QDs and transmitters as well as the energy of the spacer that triplet excitons tunnel through. For aromatic spacers such as phenylene, β varies from 0.3 to 0.7 Å⁻¹ for different QD-transmitter combinations (32, 68); for aliphatic spacers, β can be as high as 2 Å⁻¹ due to the higher energy barrier compared to that of phenylene (48). It is worth noting that when the energy barrier of spacers is comparable to the state energy of the dark, triplet-like exciton of the QD, triplet excitons hop instead of tunnel through the energy barrier, and the distance dependence decreases from exponential to ohmic (32).

3.3.3. Binding group. The anchoring group changes the dynamics of TET by means of affecting the QD-transmitter electronic coupling. First, the position of anchoring groups on transmitters determines the binding geometry that modifies the wave function overlap between QDs and transmitters (64). Two reports from the Tang group (70, 85) showed the different UC intensity with isomeric anthracene carboxylic acid as transmitters in CdSe QD-sensitized UC. This was explained by He et al. (57) as the modification of QD-transmitter coupling by transmitter binding geometry (**Figure 6***c*): The orthogonal configuration between carboxylate and anthracene in 9-ACA leads to a through-space coupling, while the coplanar configuration in 2-anthracene carboxylic acid (2-ACA) allows for the through-bond coupling. For strongly confined QDs such as CdSe, the carrier wave function amplitude is high on QD surfaces. As the anthracene moiety in 9-ACA is closer to QDs than that in 2-ACA, TET to 9-ACA is more favorable. On the contrary, for relatively weakly confined QDs such as CsPbBr₃, the carrier wave function amplitude is low on QD surfaces, and only through-bond coupling is allowed. In this case, $\eta_{\rm UC}$ with 2-ACA as the transmitter is higher.

Second, strong electronic coupling between QDs and transmitters can be achieved by selecting proper binding groups, which greatly enhance η_{TET1} and η_{UC} (31). Wang et al. (47) demonstrated that efficient Si QD-sensitized UC can be achieved with a 9-vinylanthracene transmitter ligand with η_{UC} of 8.6%, the record for the Si QD-based UC. This is attributed to the strong coupling and hybridization of valence states between anthracene and Si QDs (**Figure 6d**), as seen

DBP: dibenzotetraphenylperiflanthene in both experimental and computational studies. In the TA spectra, upon the excitation of the Si QDs, there appears a new band centered at 480 nm. This band is distinct from the molecular anthracene triplet state and assigned to delocalized mixed Si:anthracene states with triplet character. Density functional theory calculations shows that the hole and electron comprising the photogenerated triplet exciton are significantly delocalized throughout Si QDs and 9-vinylanthracene, suggesting a strong electronic coupling through the C=C bridging group. In comparison, when the π -bridge is replaced with a σ -bridge, the triplet exciton remains localized to 9-ethylanthracene, which means Si QDs and anthracene are not strongly coupled through an aliphatic C–C bridge. This work provides a new way to tailor electronic coupling between molecules and QDs through linker chemistry.

4. CHALLENGES AND FUTURE DIRECTIONS

4.1. Low $\eta_{\rm UC}$ in Solution Phase with Quantum Dot Sensitizers Compared with Molecular Sensitizers: Low $\eta_{\rm TET1}$ × $\eta_{\rm TET2}$

The highest η_{UC} sensitized by QDs is about half of that with molecular sensitizers; e.g., when comparing CdSe and PtOEP triplet photosensitizers with the same DPA emitter, $\eta_{\text{UC}} = 12\%$ for CdSe (56) compared to 27% for PtOEP (88). In another example, for the same TIPS-Nph emitter, $\eta_{\text{UC}} = 10.3\%$ with an Ir-based organometallic complex (4) compared to 5.1% with perovskite NCs (59). The difference lies in the TET from sensitizers to emitters. While η_{TET} is $\sim 100\%$ for molecular-sensitized UC, it is challenging to maximize $\eta_{\text{TET}1}$ and $\eta_{\text{TET}2}$ in QD-sensitized UC simultaneously. The equivalent η_{TET} , the product of $\eta_{\text{TET}1}$ and $\eta_{\text{TET}2}$, is far from unity. As discussed by Xu et al. (33) (**Figure 7a**), when $\eta_{\text{TET}1}$ is maximized by shortening the distance between QDs and transmitters, there is a fast quenching of transmitter triplets by QDs, rendering a low $\eta_{\text{TET}2}$; on the other hand, when transmitters are controlled to be far enough from QDs for quantitative $\eta_{\text{TET}2}$, $\eta_{\text{TET}1}$ is low. Three methods to address this issue are proposed. Firstly, precisely control the QD-transmitter distance to maximize the product of $\eta_{\text{TET}1}$ and $\eta_{\text{TET}2}$ (86). Secondly, design a transmitter-free system by using short surfactants to minimize energy barriers for Dexter energy transfer (48, 63). And lastly, use QDs based on light elements like Si (47, 79) with insignificant spin-orbit coupling.

4.2. Low $\eta_{\rm UC}$ in Solid-State Upconversion: $\eta_{\rm TTA}$ and $\eta_{\rm F}$

The application of UC in optoelectronic devices requires efficient photon UC in the solid state. However, the highest efficiency of UC films is only 3.5% (63). This is because emitters in the solid state aggregate to diminish η_{TTA} and η_{F} in UC. Specifically, molecular diffusion is hindered in the solid state, so TTA based on the triplet exciton diffusion may be slowed down, especially at grain boundaries or defects in UC films. Besides, aggregated emitters typically demonstrate concentration quenching or low emitter fluorescence QYs (low η_F) (90, 91). Furthermore, excimer formation may occur, or close packing might promote the reverse process of TTA, i.e., singlet fission. Both processes deplete emitter singlets, resulting in low η_{TTA} (92–95), which is detrimental to $\eta_{\rm UC}$. One way to overcome these challenges is to optimize the emitter design by incorporating emitters into gels, amorphous polymers, and crystalline structures, etc., which has been discussed in detail elsewhere (96). The other is to dope an energy reservoir into UC emitters. For example, ~0.5–1% dibenzotetraphenylperiflanthene (DBP) is typically used to dope rubrene layers in PbS QD-sensitized UC (Figure 7b) (21, 51, 97–99), a strategy adopted from the OLED community. As the S_1 energy of DBP is slightly lower than that of rubrene, energy can be transferred from rubrene singlets to DBP after TTA, via dipole-dipole coupling at unity efficiency. The sparsely dispersed DBP can emit photons through fluorescence efficiently.

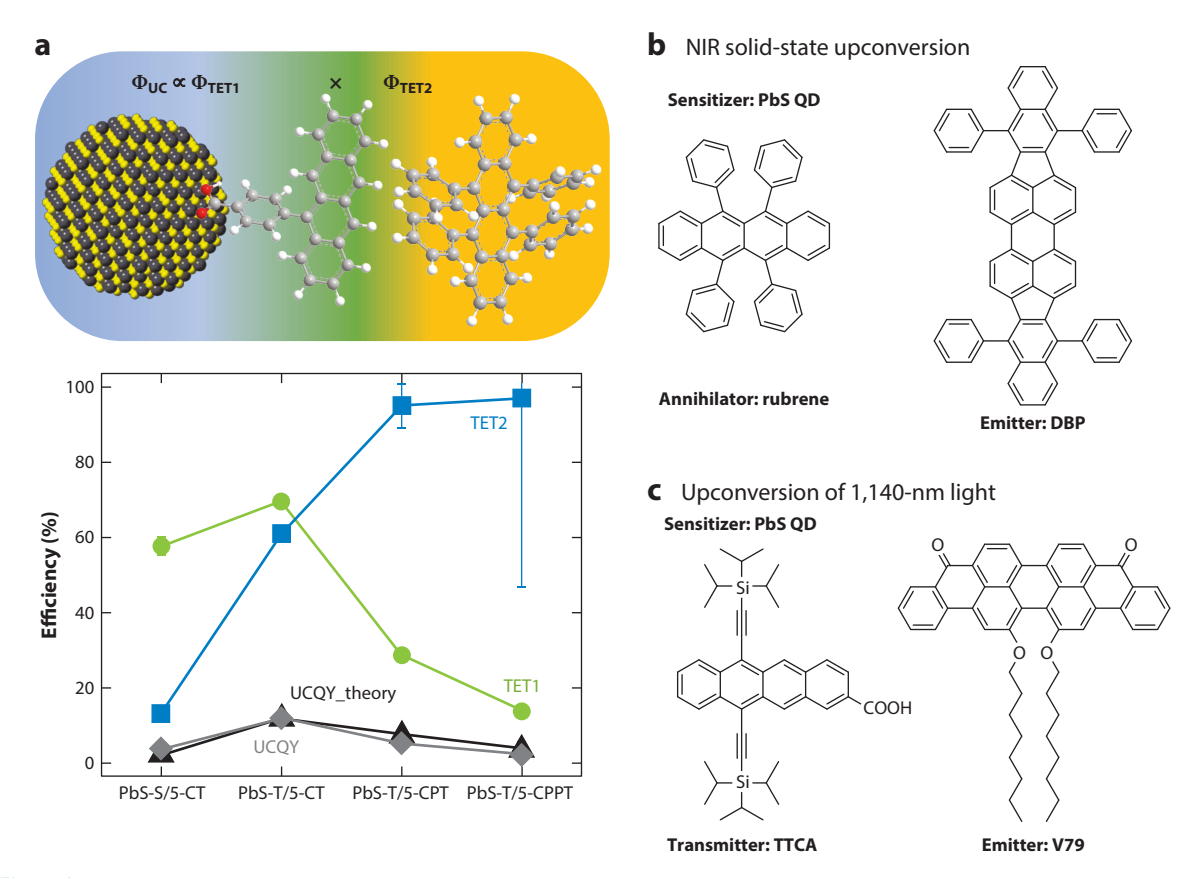


Figure 7

(a) The relationship between the efficiency of TET from QD sensitizers to transmitters, Φ_{TET2} , and the efficacy of triplet energy transfer from transmitters to emitters, Φ_{TET2} . (b) DBP is doped in the rubrene layer as the emitter in solid-state UC. (c) The UC of light beyond the Si band gap is demonstrated with PbS QD sensitizers, tetracene-based transmitters, and a violanthrone derivative as emitters. Abbreviations: DBP, dibenzotetraphenylperiflanthene; NIR, near infrared; QD, quantum dot; QY, quantum yield; TET, triplet energy transfer; TTCA, 6,11-bis(triisopropylsilylethynyl)tetracene-2-carboxylic acid; UC, upconversion. Panel a adapted with permission from Reference 33; copyright 2020 American Chemical Society.

4.3. Reabsorption and Outcoupling

QDs quench the excited singlet state of emitters in the near field, and they reabsorb the upconverted emission in the far field. Both are loss mechanisms, detrimental to $\eta_{\rm UC}$. To address the former, the strategy in solid-state UC devices is separate layers of QDs and emitters (21, 51, 58, 63, 98). Instead of mixing QDs with emitters in solution and then casting films, this strategy effectively minimizes the direct quenching of emitter S₁ by QDs, and a record efficiency of 3.5% for solid-state UC has been obtained. However, in this geometry, TET from the QD to the emitter can only occur at the QD-emitter bilayer interface, and this requires lossless triplet exciton transport within QD layers for a high η_{UC} . Since this is challenging, typically, an ultrathin QD layer with only a few monolayers is used in UC devices. Another solution would be making use of the emitter S₁ before quenching occurs. The Wu group (44) demonstrated the application of ZnScoated CuInSe₂ QD/rubrene NIR-to-visible photon UC for photocatalysis. Instead of collecting the upconverted photons, they showed that photoredox reactions can be directly triggered by the rubrene S₁ state.

4.4. Conversion of Photons Beyond the Si Band Gap Is Challenging

TES-ADT: 5,11-bis(triethylsilylethynyl)-anthradithiophene

As the photovoltaics market is still dominated by silicon, it is important to design UC devices that can harvest light beyond the Si band gap. So far, two papers have demonstrated the possibility of converting light from \sim 1,100 nm to visible wavelengths. Nishimura et al. (100) reported that PbS QDs combined with 5,11-bis(triethylsilylethynyl)anthradithiophene (TES-ADT) emitters can upconvert 1,064 nm to visible. The authors claim that the thiophene group in TES-ADT enables a close association with PbS QDs. In this system, TES-ADT serves as both transmitter and emitter. However, the $\eta_{\rm UC}$ is only 0.047%, limited by the low TET efficiency from PbS QDs to TES-ADT (8.8%) and the low fluorescence QY of TES-ADT (5.4%). Separately, Gholizadeh et al. (89) showed the UC of 1,140-nm light to visible with PbS QD sensitizers, tetracene-based transmitters, and a violanthrone-derivative emitter, as shown in **Figure 7***c*. While the use of transmitters boosts the total TET efficiency ($\eta_{\rm TET1} \times \eta_{\rm TET2}$) to be 38.3%, the $\eta_{\rm TTA}$ is only 0.65%, rendering $\eta_{\rm UC}$ to be 0.031%. Therefore, new transmitters and emitters with proper triplet energy and efficient $\eta_{\rm TTA}$ and $\eta_{\rm F}$ are needed for an efficient conversion of light with wavelengths longer than the Si band gap.

5. CONCLUSIONS

In this review, we introduced a hybrid organic-QD UC platform and reviewed the current status of this field. By enhancing TET across this organic-inorganic interface, the efficiencies of this TTA-based photon UC platform have been increased by minimizing defects in QDs and designing transmitter ligands that promote Dexter energy transfer. Nonetheless, the strong reabsorption of upconverted light by QDs, the challenge in perfectly passivating the QD surface without a thick inorganic shell, and the dearth of efficient TTA chromophores for energy conversion of midinfrared photons pose problems that need a solution. New materials and better device design are needed to for this photon UC platform to be applied in photovoltaics, photocatalysis, or biological imaging.

DISCLOSURE STATEMENT

The authors are not aware of any affiliations, memberships, funding, or financial holdings that might be perceived as affecting the objectivity of this review.

ACKNOWLEDGMENTS

Z.H. acknowledges support from the National Key Research and Development Program of China (2022YFA1502900), the National Natural Science Foundation of China (22231001), and the Chinese Academy of Science Project for Young Scientists in Basic Research (YSBR-094). M.L.T. acknowledges support from the US Department of Energy, Office of Science, Office of Basic Energy Sciences, Solar Photochemistry Program Project (DE-SC0022523). This review is based on work supported by Air Force of Scientific Research award FA9550-20-1-0112 to M.L.T., as well as National Science Foundation award CHE-2147792.



LITERATURE CITED

- Tasaki S, Nishimura K, Toyoshima H, Masuda T, Nakamura M, et al. 2022. Realization of ultra-highefficient fluorescent blue OLED. J. Soc. Inf. Disp. 30:441–51
- 2. Kondakov DY, Pawlik TD, Hatwar TK, Spindler JP. 2009. Triplet annihilation exceeding spin statistical limit in highly efficient fluorescent organic light-emitting diodes. *J. Appl. Phys.* 106:124510
- Di DW, Yang L, Richter JM, Meraldi L, Altamimi RM, et al. 2017. Efficient triplet exciton fusion in molecularly doped polymer light-emitting diodes. *Adv. Mater.* 29:1605987

- 4. Harada N, Sasaki Y, Hosoyamada M, Kimizuka N, Yanai N. 2021. Discovery of key TIPS-naphthalene for efficient visible-to-UV photon upconversion under sunlight and room light. Angew. Chem. Int. Ed. 60:142-47
- 5. Mahboub M, Huang Z, Tang ML. 2016. Efficient infrared-to-visible upconversion with subsolar irradiance. Nano Lett. 16:7169-75
- 6. Chen S, Weitemier AZ, Zeng X, He LM, Wang XY, et al. 2018. Near-infrared deep brain stimulation via upconversion nanoparticle-mediated optogenetics. Science 359:679-83
- 7. Chan EM. 2015. Combinatorial approaches for developing upconverting nanomaterials: highthroughput screening, modeling, and applications. Chem. Soc. Rev. 44:1653-79
- 8. Dong H, Du SR, Zheng XY, Lyu GM, Sun LD, et al. 2015. Lanthanide nanoparticles: from design toward bioimaging and therapy. Chem. Rev. 115:10725-815
- Cosco ED, Caram JR, Bruns OT, Franke D, Day RA, et al. 2017. Flavylium polymethine fluorophores for near- and shortwave infrared imaging. Angew. Chem. Int. Ed. 56:13126-29
- 10. Parker CA, Hatchard CG. 1962. Sensitised anti-Stokes delayed fluorescence. Proc. Chem. Soc. Lond. 1962:386-87
- 11. Parker CA. 1963. Sensitized P-type delayed fluorescence. Proc. R. Soc. Lond. A 276:125-35
- 12. Keivanidis PE, Baluschev S, Miteva T, Nelles G, Scherf U, et al. 2003. Up-conversion photoluminescence in polyfluorene doped with metal (II)-octaethyl porphyrins. Adv. Mater. 15:2095-98
- 13. Baluschev S, Keivanidis PE, Wegner G, Jacob J, Grimsdale AC, et al. 2005. Upconversion photoluminescence in poly(ladder-type-pentaphenylene) doped with metal (II)-octaethyl porphyrins. Appl. Phys. Lett. 86:061904
- 14. Yakutkin V, Aleshchenkov S, Chernov S, Miteva T, Nelles G, et al. 2008. Towards the IR limit of the triplet-triplet annihilation-supported up-conversion: tetraanthraporphyrin. Chemistry 14:9846-50
- 15. Amemori S, Sasaki Y, Yanai N, Kimizuka N. 2016. Near-infrared-to-visible photon upconversion sensitized by a metal complex with spin-forbidden yet strong S_0 - T_1 absorption. J. Am. Chem. Soc. 138:8702-5
- 16. Monguzzi A, Tubino R, Hoseinkhani S, Campione M, Meinardi F. 2012. Low power, non-coherent sensitized photon up-conversion: modelling and perspectives. Phys. Chem. Chem. Phys. 14:4322-32
- 17. Schmidt TW, Castellano FN. 2014. Photochemical upconversion: the primacy of kinetics. 7. Phys. Chem. Lett. 5:4062-72
- 18. Tabachnyk M, Ehrler B, Gelinas S, Bohm ML, Walker BJ, et al. 2014. Resonant energy transfer of triplet excitons from pentacene to PbSe nanocrystals. Nat. Mater. 13:1033-38
- 19. Thompson NJ, Wilson MWB, Congreve DN, Brown PR, Scherer JM, et al. 2014. Energy harvesting of non-emissive triplet excitons in tetracene by emissive PbS nanocrystals. Nat. Mater. 13:1039-43
- 20. Nirmal M, Norris DJ, Kuno M, Bawendi MG, Efros AL, Rosen M. 1995. Observation of the "dark exciton" in CdSe quantum dots. Phys. Rev. Lett. 75:3728-31
- 21. Wu M, Congreve DN, Wilson MWB, Jean J, Geva N, et al. 2016. Solid-state infrared-to-visible upconversion sensitized by colloidal nanocrystals. Nat. Photon. 10:31-34
- 22. Mongin C, Moroz P, Zamkov M, Castellano FN. 2018. Thermally activated delayed photoluminescence from pyrenyl-functionalized CdSe quantum dots. Nat. Chem. 10:225-30
- 23. Biadala L, Siebers B, Bevazit Y, Tessier MD, Dupont D, et al. 2016. Band-edge exciton fine structure and recombination dynamics in InP/ZnS colloidal nanocrystals. ACS Nano 10:3356-64
- 24. Sercel PC, Efros AL. 2018. Band-edge exciton in CdSe and other II-VI and III-V compound semiconductor nanocrystals - revisited. Nano Lett. 18:4061-68
- 25. Diroll BT, Schaller RD. 2019. Thermal excitation control over photon emission rate of CdSe nanocrystals. Nano Lett. 19:2322-28
- 26. Schaller RD, Crooker SA, Bussian DA, Pietryga JM, Joo J, Klimov VI. 2010. Revealing the exciton fine structure of PbSe nanocrystal quantum dots using optical spectroscopy in high magnetic fields. Phys. Rev. Lett. 105:067403
- 27. Brovelli S, Schaller RD, Crooker SA, Garcia-Santamaria F, Chen Y, et al. 2011. Nano-engineered electron-hole exchange interaction controls exciton dynamics in core-shell semiconductor nanocrystals. Nat. Commun. 2:280

ARjats.cls

- 28. Reboredo FA, Franceschetti A, Zunger A. 2000. Dark excitons due to direct Coulomb interactions in silicon quantum dots. Phys. Rev. B 61:13073-87
- 29. Jin T, He S, Zhu YF, Egap E, Lian TQ. 2022. Bright state sensitized triplet energy transfer from quantum dot to molecular acceptor revealed by temperature dependent energy transfer dynamics. Nano Lett. 22:3897-903
- 30. Skourtis SS, Liu CR, Antoniou P, Virshup AM, Beratan DN. 2016. Dexter energy transfer pathways. PNAS 113:8115-20
- 31. De Roo J, Huang Z, Schuster NJ, Hamachi LS, Congreve DN, et al. 2020. Anthracene diphosphate ligands for CdSe quantum dots; molecular design for efficient upconversion. Chem. Mater. 32:1461-66
- 32. Huang Z, Xu Z, Huang T, Gray V, Moth-Poulsen K, et al. 2020. Evolution from tunneling to hopping mediated triplet energy transfer from quantum dots to molecules. J. Am. Chem. Soc. 142:17581-88
- 33. Xu Z, Huang Z, Li C, Huang T, Evangelista FA, et al. 2020. Tuning the quantum dot (QD)/mediator interface for optimal efficiency of QD-sensitized near-infrared-to-visible photon upconversion systems. ACS Appl. Mater. Interfaces 12:36558-67
- 34. Huang Z, Xu Z, Mahboub M, Li X, Taylor JW, et al. 2017. PbS/CdS core-shell quantum dots suppress charge transfer and enhance triplet transfer. Angew. Chem. Int. Ed. 56:16583-87
- 35. Garakyaraghi S, Mongin C, Granger DB, Anthony JE, Castellano FN. 2017. Delayed molecular triplet generation from energized lead sulfide quantum dots. J. Phys. Chem. Lett. 8:1458-63
- 36. Papa CM, Garakyaraghi S, Granger DB, Anthony JE, Castellano FN. 2020. TIPS-pentacene triplet exciton generation on PbS quantum dots results from indirect sensitization. Chem. Sci. 11:5690-96
- 37. Köhler A, Bässler H. 2011. What controls triplet exciton transfer in organic semiconductors? *J. Mater.* Chem. 21:4003-11
- 38. Olshansky JH, Ding TX, Lee YV, Leone SR, Alivisatos AP. 2015. Hole transfer from photoexcited quantum dots: the relationship between driving force and rate. 7. Am. Chem. Soc. 137:15567-75
- 39. Chen XK, Kim D, Bredas JL. 2018. Thermally activated delayed fluorescence (TADF) path toward efficient electroluminescence in purely organic materials: molecular level insight. Acc. Chem. Res. 51:2215-
- 40. Uoyama H, Goushi K, Shizu K, Nomura H, Adachi C. 2012. Highly efficient organic light-emitting diodes from delayed fluorescence. Nature 492:234-38
- 41. Zhang XG, Castellano FN. 2022. Thermally activated bright-state delayed blue photoluminescence from InP quantum dots. J. Phys. Chem. Lett. 13:3706-11
- 42. Zhang XA, Hudson MH, Castellano FN. 2022. Engineering long-lived blue photoluminescence from InP quantum dots using isomers of naphthoic acid. 7. Am. Chem. Soc. 144:3527-34
- 43. VanOrman ZA, Weiss R, Bieber AS, Chen B, Nienhaus L. 2023. Mechanistic insight into CdSe nanoplatelet-sensitized upconversion: size and stacking induced effects. Chem. Commun. 59:322-25
- 44. Liang W, Nie C, Du J, Han Y, Zhao G, et al. 2023. Near-infrared photon upconversion and solar synthesis using lead-free nanocrystals. Nat. Photon. 17:346-53
- 45. Jaimes P, Miyashita T, Qiao T, Wang K, Tang ML. 2023. Photon upconversion in the visible wavelengths with ZnSe/InP/ZnS nanocrystals. J. Phys. Chem. C 127:1752-57
- 46. Gong N, Xu B, Mo J, Man T, Qiu J. 2023. Defect engineering of inorganic sensitizers for efficient triplet-triplet annihilation upconversion. Trends Chem. 5:295-311
- Wang K, Cline RP, Schwan J, Strain JM, Roberts ST, et al. 2023. Efficient photon upconversion enabled by strong coupling between silicon quantum dots and anthracene. Nat. Chem. 15:1172-78
- 48. Miyashita T, Jaimes P, Lian T, Tang ML, Xu Z. 2022. Quantifying the ligand-induced triplet energy transfer barrier in a quantum dot-based upconversion system. J. Phys. Chem. Lett. 13:3002-7
- 49. Lin X, Chen Z, Han Y, Nie C, Xia P, et al. 2022. ZnSe/ZnS core/shell quantum dots as triplet sensitizers toward visible-to-ultraviolet B photon upconversion. ACS Energy Lett. 7:914-19
- 50. Gray V, Drake W, Allardice JR, Zhang Z, Xiao J, et al. 2022. Triplet transfer from PbS quantum dots to tetracene ligands: Is faster always better? 7. Mater. Chem. C 10:16321-29
- 51. Wu M, Lin T-A, Tiepelt JO, Bulović V, Baldo MA. 2021. Nanocrystal-sensitized infrared-to-visible upconversion in a microcavity under subsolar flux. Nano Lett. 21:1011-16
- 52. VanOrman ZA, Conti CR III, Strouse GF, Nienhaus L. 2021. Red-to-blue photon upconversion enabled by one-dimensional CdTe nanorods. Chem. Mater. 33:452-58

February 8, 2024

- 53. Koharagi M, Harada N, Okumura K, Miyano J, Hisamitsu S, et al. 2021. Green-to-UV photon upconversion enabled by new perovskite nanocrystal-transmitter-emitter combination. Nanoscale 13:19890-93
- 54. Zhang J, Kouno H, Yanai N, Eguchi D, Nakagawa T, et al. 2020. Number of surface-attached acceptors on a quantum dot impacts energy transfer and photon upconversion efficiencies. ACS Photon. 7:1876-84
- 55. VanOrman ZA, Bieber AS, Wieghold S, Nienhaus L. 2020. Green-to-blue triplet fusion upconversion sensitized by anisotropic CdSe nanoplatelets. Chem. Mater. 32:4734-42
- 56. Ronchi A, Capitani C, Pinchetti V, Gariano G, Zaffalon ML, et al. 2020. High photon upconversion efficiency with hybrid triplet sensitizers by ultrafast hole-routing in electronic-doped nanocrystals. Adv. Mater. 32:2002953
- 57. He S, Lai R, Jiang Q, Han Y, Luo X, et al. 2020. Engineering sensitized photon upconversion efficiency via nanocrystal wavefunction and molecular geometry. Angew. Chem. Int. Ed. 59:17726-31
- 58. Nienhaus L, Correa-Baena J-P, Wieghold S, Einzinger M, Lin T-A, et al. 2019. Triplet-sensitization by lead halide perovskite thin films for near-infrared-to-visible upconversion. ACS Energy Lett. 4:888–95
- 59. He S, Luo X, Liu X, Li YL, Wu KF. 2019. Visible-to-ultraviolet upconversion efficiency above 10% sensitized by quantum-confined perovskite nanocrystals. J. Phys. Chem. Lett. 10:5036-40
- 60. Han Y, He S, Luo X, Li Y, Chen Z, et al. 2019. Triplet sensitization by "self-trapped" excitons of nontoxic CuInS₂ nanocrystals for efficient photon upconversion. J. Am. Chem. Soc. 141:13033–37
- 61. Mahboub M, Xia P, Van Baren J, Li X, Lui CH, Tang ML. 2018. Midgap states in PbS quantum dots induced by Cd and Zn enhance photon upconversion. ACS Energy Lett. 3:767-72
- 62. Huang ZY, Xia P, Megerdich N, Fishman DA, Vullev VI, Tang ML. 2018. ZnS shells enhance triplet energy transfer from CdSe nanocrystals for photon upconversion. ACS Photon. 5:3089–96
- Nienhaus L, Wu M, Geva N, Shepherd JJ, Wilson MWB, et al. 2017. Speed limit for triplet-exciton transfer in solid-state PbS nanocrystal-sensitized photon upconversion. ACS Nano 11:7848-57
- 64. Li X, Fast A, Huang Z, Fishman DA, Tang ML. 2017. Complementary lock-and-key ligand binding of a triplet transmitter to a nanocrystal photosensitizer. Angew. Chem. Int. Ed. 56:5598-602
- 65. Gray V, Xia P, Huang Z, Moses E, Fast A, et al. 2017. CdS/ZnS core-shell nanocrystal photosensitizers for visible to UV upconversion. Chem. Sci. 8:5488–96
- 66. Okumura K, Mase K, Yanai N, Kimizuka N. 2016. Employing core-shell quantum dots as triplet sensitizers for photon upconversion. Chemistry 22:7721–26
- 67. Mahboub M, Maghsoudiganjeh H, Pham AM, Huang Z, Tang ML. 2016. Triplet energy transfer from PbS(Se) nanocrystals to rubrene: the relationship between the upconversion quantum yield and size. Adv. Funct. Mater. 26:6091-97
- 68. Li X, Huang Z, Zavala R, Tang ML. 2016. Distance-dependent triplet energy transfer between CdSe nanocrystals and surface bound anthracene. J. Phys. Chem. Lett. 7:1955-59
- 69. Huang Z, Simpson DE, Mahboub M, Li X, Tang ML. 2016. Ligand enhanced upconversion of nearinfrared photons with nanocrystal light absorbers. Chem. Sci. 7:4101-4
- 70. Huang Z, Li X, Mahboub M, Hanson KM, Nichols VM, et al. 2015. Hybrid molecule-nanocrystal photon upconversion across the visible and near-infrared. Nano Lett. 15:5552-57
- 71. Huang Z, Li X, Yip BD, Rubalcava JM, Bardeen CJ, Tang ML. 2015. Nanocrystal size and quantum yield in the upconversion of green to violet light with CdSe and anthracene derivatives. Chem. Mater. 27:7503-7
- 72. Rigsby EM, Miyashita T, Jaimes P, Fishman DA, Tang ML. 2020. On the size-dependence of CdSe nanocrystals for photon upconversion with anthracene. 7. Chem. Phys. 153:114702
- 73. Amemori S, Gupta RK, Bohm ML, Xiao J, Huynh U, et al. 2018. Hybridizing semiconductor nanocrystals with metal-organic frameworks for visible and near-infrared photon upconversion. Dalton Trans. 47:8590-94
- 74. Lai RC, Sang YB, Zhao Y, Wu KF. 2020. Triplet sensitization and photon upconversion using InP-based quantum dots. 7. Am. Chem. Soc. 142:19825-29
- 75. Mase K, Okumura K, Yanai N, Kimizuka N. 2017. Triplet sensitization by perovskite nanocrystals for photon upconversion. Chem. Commun. 53:8261-64
- 76. Tripathi N, Ando M, Akai T, Kamada K. 2021. Efficient NIR-to-visible upconversion of surfacemodified PbS quantum dots for photovoltaic devices. ACS Appl. Nano Mater. 4:9680-88

ARjats.cls

- 77. Wu MF, Jean J, Bulovic V, Baldo MA. 2017. Interference-enhanced infrared-to-visible upconversion in solid-state thin films sensitized by colloidal nanocrystals. Appl. Phys. Lett. 110:211101
- 78. Xia P, Schwan J, Dugger TW, Mangolini L, Tang ML. 2021. Air-stable silicon nanocrystal-based photon upconversion. Adv. Opt. Mater. 9:2100453
- 79. Xia P, Raulerson EK, Coleman D, Gerke CS, Mangolini L, et al. 2020. Achieving spin-triplet exciton transfer between silicon and molecular acceptors for photon upconversion. Nat. Chem. 12:137-44
- 80. Murov SL, Carmichael I, Hug GL. 1993. Handbook of Photochemistry. Boca Raton, FL: CRC Press
- 81. Zhao G, Chen Z, Xiong K, Liang G, Zhang J, Wu K. 2021. Triplet energy migration pathways from PbS quantum dots to surface-anchored polyacenes controlled by charge transfer. Nanoscale 13:1303-10
- 82. Bender JA, Raulerson EK, Li X, Goldzak T, Xia P, et al. 2018. Surface states mediate triplet energy transfer in nanocrystal-acene composite systems. J. Am. Chem. Soc. 140:7543-53
- 83. Jin T, Lian T. 2020. Trap state mediated triplet energy transfer from CdSe quantum dots to molecular acceptors. 7. Chem. Phys. 153:074703
- 84. Huang Z, Xia P, Megerdich N, Fishman DA, Vullev VI, Tang ML. 2018. ZnS shells enhance triplet energy transfer from CdSe nanocrystals for photon upconversion. ACS Photon. 5:3089–96
- 85. Xia P, Huang Z, Li X, Romero JJ, Vullev VI, et al. 2017. On the efficacy of anthracene isomers for triplet transmission from CdSe nanocrystals. Chem. Commun. 53:1241-44
- 86. Xu Z, Huang Z, Jin T, Lian T, Tang ML. 2021. Mechanistic understanding and rational design of quantum dot/mediator interfaces for efficient photon upconversion. Acc. Chem. Res. 54:70–80
- 87. Tabachnyk M, Ehrler B, Gélinas S, Böhm ML, Walker BJ, et al. 2014. Resonant energy transfer of triplet excitons from pentacene to PbSe nanocrystals. Nat. Mater. 13:1033–38
- 88. Nishimura N, Gray V, Allardice JR, Zhang Z, Pershin A, et al. 2019. Photon upconversion from nearinfrared to blue light with TIPS-anthracene as an efficient triplet-triplet annihilator. ACS Mater. Lett.
- Gholizadeh EM, Prasad SKK, Teh ZL, Ishwara T, Norman S, et al. 2020. Photochemical upconversion of near-infrared light from below the silicon bandgap. Nat. Photon. 14:585-90
- Chandross EA, Dempster CJ. 1970. Intramolecular excimer formation and fluorescence quenching in dinaphthylalkanes. J. Am. Chem. Soc. 92:3586-93
- 91. Mei J, Leung NLC, Kwok RTK, Lam JWY, Tang BZ. 2015. Aggregation-induced emission: Together we shine, united we soar! Chem. Rev. 115:11718-940
- 92. Ye C, Gray V, Mårtensson J, Börjesson K. 2019. Annihilation versus excimer formation by the triplet pair in triplet-triplet annihilation photon upconversion. J. Am. Chem. Soc. 141:9578-84
- Yong CK, Musser AJ, Bayliss SL, Lukman S, Tamura H, et al. 2017. The entangled triplet pair state in acene and heteroacene materials. Nat. Commun. 8:15953
- 94. Zhao W, Castellano FN. 2006. Upconverted emission from pyrene and di-tert-butylpyrene using Ir(ppy)₃ as triplet sensitizer. 7. Phys. Chem. A 110:11440-45
- 95. Olesund A, Gray V, Mårtensson J, Albinsson B. 2021. Diphenylanthracene dimers for triplet-triplet annihilation photon upconversion: mechanistic insights for intramolecular pathways and the importance of molecular geometry. 7. Am. Chem. Soc. 143:5745-54
- 96. Alves J, Feng J, Nienhaus L, Schmidt TW. 2022. Challenges, progress and prospects in solid state triplet fusion upconversion. J. Mater. Chem. C 10:7783-98
- 97. Perkinson CF, Einzinger M, Finley J, Bawendi MG, Baldo MA. 2022. Magnetic-field-switchable laser via optical pumping of rubrene. Adv. Mater. 34:2103870
- Wang L, Yoo JJ, Lin T-A, Perkinson CF, Lu Y, et al. 2021. Interfacial trap-assisted triplet generation in lead halide perovskite sensitized solid-state upconversion. Adv. Mater. 33:2100854
- 99. Wieghold S, Bieber AS, VanOrman ZA, Rodriguez A, Nienhaus L. 2020. Is disorder beneficial in perovskite-sensitized solid-state upconversion? the role of DBP doping in rubrene. 7. Phys. Chem. C 124:18132-40
- 100. Nishimura N, Allardice JR, Xiao J, Gu Q, Gray V, Rao A. 2019. Photon upconversion utilizing energy beyond the band gap of crystalline silicon with a hybrid TES-ADT/PbS quantum dots system. Chem. Sci. 10:4750-60